Pergamon

Tetrahedron 56 (2000) 1197–1206

TETRAHEDRON

Synthesis of 4-Thiothymine Based Photolabels as New Tools for Nucleic Acids Structural Studies in Solution: Formation of Long-Range Photo-Cross-Links within a Hammerhead Ribozyme Domain

Carole Saintomé,[a,b,†] Pascale Clivio,[a,*] Jean-Louis Fourrey,[a] Anne Woisard,[b] Philippe Laugâa[b] and Alain Favre[b]

[a]*Institut de Chimie des Substances Naturelles, CNRS, 91198 Gif-sur-Yvette, France*

[b]*Laboratoire de Photobiologie Moléculaire, Institut Jacques Monod, CNRS, Universités Paris 6 et Paris 7, 2 Place Jussieu, 75251 Paris Cedex 05, France*

Received 15 October 1999; accepted 23 December 1999

Abstract—The nucleosidic photolabels **2**–**5**, able to form long-range photo-cross-links, have been used to further investigate the tertiary folding of a hammerhead ribozyme domain. These photolabels derive from 2′-deoxyuridine which is substituted at its C-5 position with a photoactivable 4-thiothymine unit linked by a chain of various length and rigidity. Derivatives **2**–**5** were inserted at strategic positions of a deoxysubstrate analogue (**dS**) of a hammerhead ribozyme (**Rz**). Covalent cross-links were generated by 366 nm irradiation of the **Rz**–**dS** complexes assembled under cleavage conditions. The **Rz** residues involved in these cross-links were mapped to give new sets of proximity data extending those previously obtained by intrinsic photolabelling with 2′-deoxy-4-thiouridine **1**. Thus, compared to the zero-length cross-linker **1**, photolabels **2**–**5** exhibit a higher exploration capacity which depends critically upon the length and flexibility of the linker and their site of incorporation. Interestingly, in contrast to **1**, these photolabels were able to cross-link residues involved in the double G:A mismatch as well as residues of the adjacent base pairs. These findings suggest that the mismatch domain exhibits an unexpected conformational flexibility in solution.

Introduction

Because of their remarkable endonuclease activity great attention is currently paid to hammerhead ribozymes.[1] When combined with their RNA substrate, these RNA molecules form a triple junction with the three double-stranded stems, I, II and III, connected to a core of conserved residues which are essential for catalytic activity. The crystal structures of two bipartite hammerhead ribozyme domains have been solved.[2] In both cases, the system adopts a Y-shaped structure with stems I and II side by side, in agreement with the results derived from the conformation studies in solution.[3–5] However, in the crystal structure, the conformation at the cleavage site does not allow an in-line attack of the scissile phosphodiester bond by the adjacent deprotonated 2′-hydroxyl as shown by the experimental data.[6] In order to approach the problem of the solution structure of a hammerhead domain, we have taken advantage of the photo-cross-linking ability of thionucleosides, such as 2′-deoxy-4-thiouridine (ds^4U)[7] **1** and 2′-deoxy-6-thioinosine (ds^6I).[8] These nucleosides were incorporated at selected positions of an all-deoxy ribozyme substrate analogue in place of thymidine to be irradiated in the presence of a 35-mer ribozyme. These photoaffinity studies allowed the identification of contacts between residues of the substrate cleavage site and residues of the 5′-conserved region of the ribozyme. Evidence for interactions between the 3′-end of the substrate and the stem loop II has also been obtained by this method. A three dimensional structure accounting for these proximity data has been modelled.[9] This model is not only in good overall agreement with the crystalline structure but, additional studies revealing that cross-links within complexes involving cleavable deoxysubstrate analogues retained activity, underlined its biological significance.[10] On the other hand, whereas crystallographic studies showed magnesium ions to induce a weak conformational motion of the catalytic core,[11] it was subsequently suggested that more important conformational changes in the global crystalline structure were needed to reach the active conformation.[12]

In order to gain further informative data on the conformational mobility of the hammerhead ribozyme domain, we

Keywords: photolabels; hammerhead ribozyme; nucleic acids.

* Corresponding author. Fax: +33-1-69-07-72-47;
e-mail: pascale.clivio@icsn.cnrs-gif.fr

† Fax: +33-1-44-27-35-80; e-mail: saintome@jim.jussieu.fr

0040–4020/00/$ - see front matter
PII: S0040-4020(00)00024-7

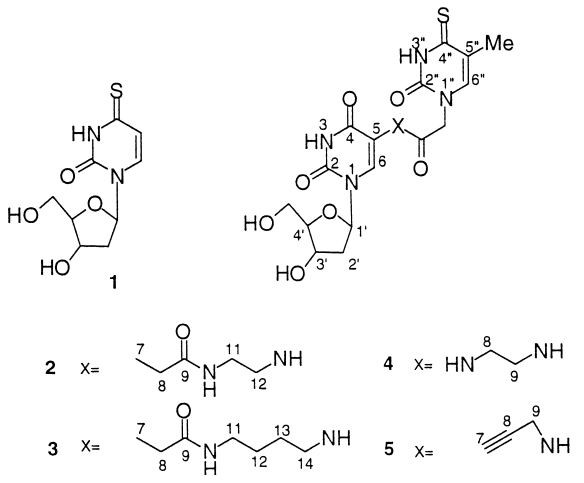

Figure 1. Structure of modified nucleosides **1**–**5**.

have synthesized a new series of photoactivable oligodeoxynucleotide probes. These probes consist of 14-mer substrate analogues **dS** of the 35-mer ribozyme **Rz** incorporating the modified 2′-deoxyuridine units **2**–**5** (Fig. 1)[13] whose photo-cross-linking abilities have already been tested in a double helix context.[14] Herein, we describe the preparation of **2**–**5** along with their incorporation into oligonucleotide probes and establish their capacity to serve as valuable structural tools to investigate the hammerhead ribozyme domain folding.

Results and Discussion

Synthesis of photolabelled deoxysubstrate analogues

The preparation of the suitably protected phosphoramidites **18a**, **18b**, **19** and **20** (Scheme 1) is a prerequisite for a convenient incorporation of nucleosides **2**–**5** into

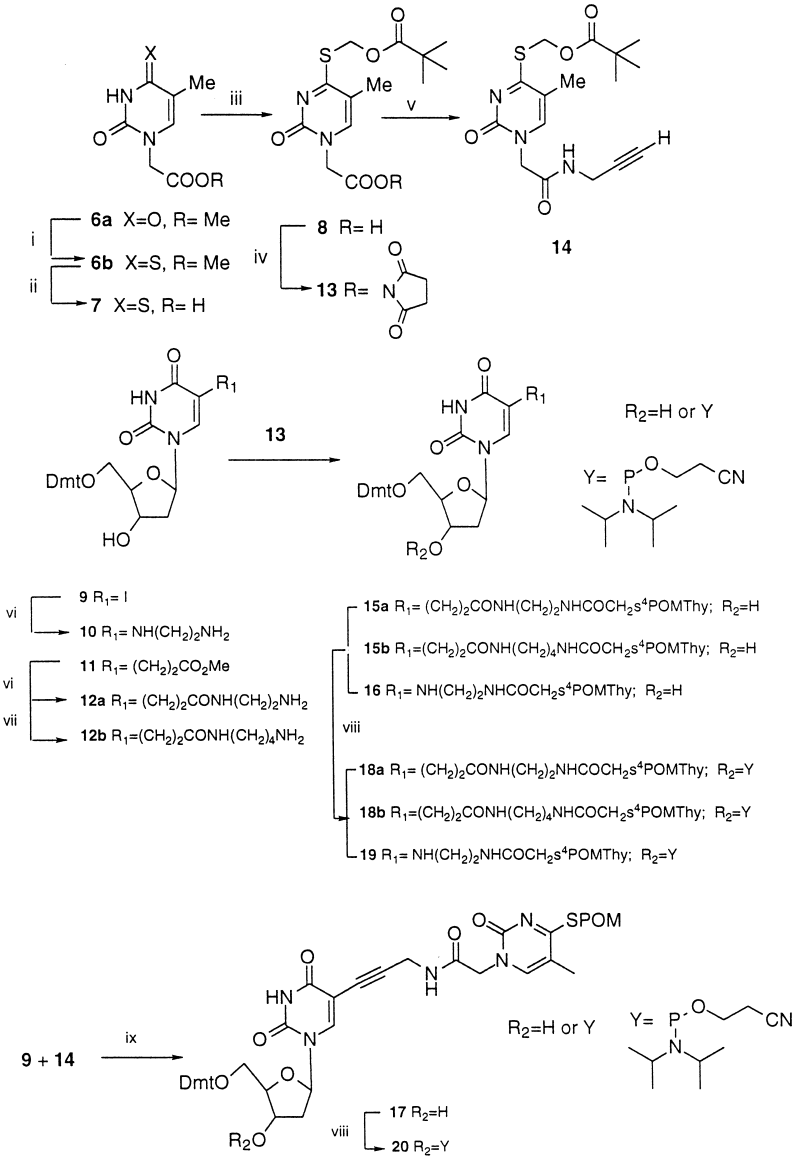

Scheme 1. (i) Phosphorus pentasulfide; (ii) 2N aqueous NaOH, H_3O^+; (iii) Pivaloyloxymethyl chloride, K_2CO_3; (iv) DCC, *N*-hydroxysuccinimide; (v) Propargylamine; (vi) Ethylenediamine; (vii) 1,4-Diaminobutane; (viii) 2-Cyanoethyl *N*,*N*-diisopropylchlorophosphoramidite, *N*,*N*-diisopropylethylamine; (ix) $(Ph_3P)_4Pd$, CuI, triethylamine.

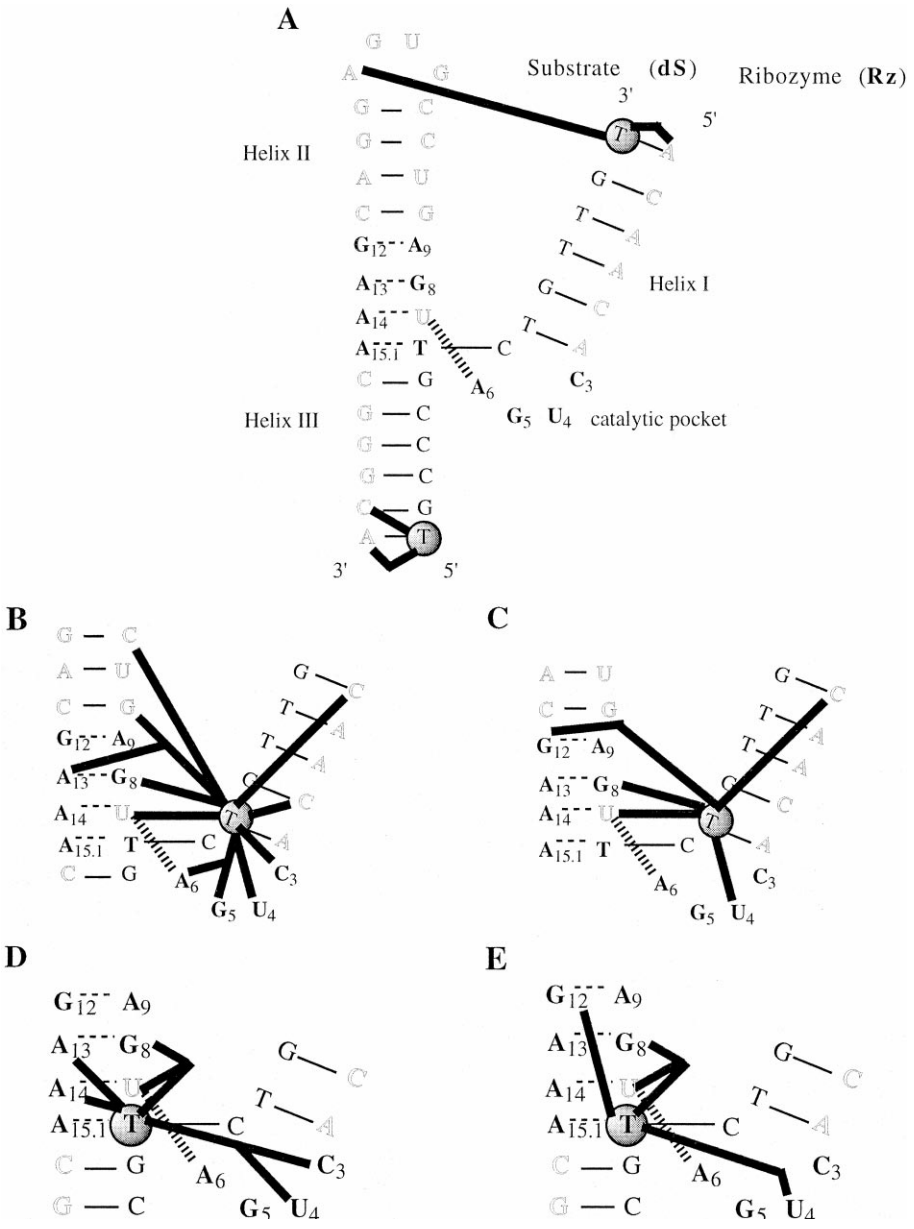

Figure 2. Ribozyme residues involved in cross-links. (Conserved residues are indicated in bold letters, variable residues of **Rz** are in outlined letters and photolabelled nucleosides are circled.) **A**: Structure of the hammerhead ribozyme domain with nucleoside **4** at positions 1.6 and 16.7 on **dS**; **B**: Nucleoside **2** at position 1.1; **C**: Nucleoside **5** at position 1.1; **D**: Nucleoside **2** at position 16.1; **E**: Nucleoside **5** at position 16.1. For ribozyme domain numbering see: *Nucleic Acids Res.* **1992**, *20*, 3252.

oligonucleotides by chemical synthesis. Intermediates **15a**, **15b** and **16**, the immediate precursors of **18a**,**b** and **19**, were obtained by acylation of an amino substrate by **13**, an activated derivative of acid **8**. Thus, the amino-nucleosides **12a**[15] and **12b**, prepared by trans-amination of the ester function of the known intermediate **11**[15] with ethylene diamine or 1,4-diaminobutane (90% yield), were treated with **13**, obtained by means of standard reactions, to give amides **15a** (77% yield) and **15b** (34% yield), respectively. In the case of **16**, nucleoside **10** was first obtained in 70% yield by overnight treatment of **9**[16] in ethylenediamine. Compound **10** was subsequently acylated by **13** to provide **16** (54% yield).

A more convergent route was defined for the preparation of nucleoside **17**. Indeed, treatment of propargylamine with **13** gave amide **14** (50% yield) which upon reaction with **9** according to Hobbs[17] and Tong,[18] provided **17** (44% yield). Nucleosides **15a**, **15b**, **16** and **17** were subsequently treated with 2-cyanoethyl *N*,*N*-diisopropylchlorophosphoramidite to give the corresponding phosphoramidites **18a**, **18b**, **19** and **20**. The latter were used to prepare 12 photolabelled analogues **dS** of the ribozyme substrate **Rz** containing at position 1.1, 1.6, 16.1 and 16.7, in place of thymidine, one of the four modified 2′-deoxyuridines **2**–**5** (Fig. 1).

Photolabelling studies of a hammerhead ribozyme domain

Cross-linking characterizations. The herein studied hammerhead ribozyme domain consisted of a 35-mer (or 36-mer) ribozyme **Rz** and its 14-mer (or 15-mer) substrate

analogue **dS**[7] containing one of the photolabels **2**–**5** inserted at a specific position (Fig. 2). The folding of this system has been previously studied using the parent 2′-deoxy-4-thiouridine **1** as zero-length photo-cross-linker.[7] Moreover, in the presence of 14-mer deoxysubstrates containing a ribocytidine at the cleavage site, **Rz** was shown to exhibit closely similar cleavage activities with respect to its all-RNA 14-mer substrate.[7,8] In the present study, photolabels **2**–**5** were site-specifically inserted at positions either 1.1 or 16.1 of **dS** adjacent to the putative cleavage site to allow exploration of the central core, whereas the two shorter ones, **4** and **5**, were also introduced at the 5′ (16.7) and 3′ (1.6) ends of **dS** (Fig. 2).

In all experiments, an excess of each **dS** (1.2 μM) was combined with 0.2 μM 5′-^{32}P-labelled **Rz** in the cleavage buffer in the presence of Mg^{2+}. The mixtures were irradiated at 15°C with 366 nm light to completion of the reaction to give intermolecular **Rz**–**dS** cross-links which were separated from each other and from unreacted **Rz** by denaturing PAGE-8 M urea. Controls indicated that there were no such reactions in the dark, neither when the complex was irradiated in the absence of Mg^{2+} nor in the presence of unmodified **dS**. Long separating gels (40 cm) were used since in some cases (with photolabels **2** and **3** at positions 1.1 and 16.1) up to 15 distinct cross-linked species were detected (Fig. 3). These species were isolated, repurified if necessary, and sequenced as previously described.[7,8,19] With a few exceptions, which may represent either mixtures of cross-linked species or chemically unstable cross-linked structures under alkaline conditions, each of these species yielded clear-cut windows on the sequencing gel allowing the determination of the ribozyme residues involved in the cross-links. In a few cases, two closely migrating cross-linked species were shown to covalently bind the same ribozyme residue. These doublet species may be due to distinct or isomeric photoadducts as previously discussed.[19] For each **dS**, the efficiency of cross-linking formation and their localizations on **Rz** have been collected in Tables 1 and 2, which also show the results previously obtained with ds^{4}U **1**, for comparison.[7]

Structural implications of the cross-links. As expected, the cross-linking efficiency and the positions of the residues of **Rz** involved in the cross-links vary according to the type of photolabel considered as well as its position within the **dS** sequence. The overall cross-linking efficiency (1–17%) is usually two to three times lower than that observed with ds^{4}U **1**.[7] This is likely due to the fact that the 4-thiothymine substituted photolabel explores a larger space allowing it to yield intramolecular cross-links with residues of the substrate analogue[14] as well as to photolytic decomposition.

In view of interpreting the cross-link data in relation to the crystalline[2c] and solution[9] structures, several points should be considered: (a) one should keep in mind that, for labels **2**–**5**, the 4-thiothymine reactive C–S bond is expected to explore a space ranging from 3.5 to 15.5 Å (**2**), 3.5–18 Å (**3**), 4.5–12 Å (**4**), 7–12 Å (**5**), from the C-5 centre of the 2′-deoxyuridine moiety;[20] (b) the distances between **Rz**–**dS** cross-linked residues can be evaluated from the presumed reactive sites as revealed in model reactions (C-5;C-6 double bond for U and C, N-7;C-8 double bond for A).[21,22] These distances were measured, in the crystalline[2c] and solution[9] structures, between the C-5 position of the substituted residue and the middle of the target double bond of the **Rz** residue involved in each cross-link (Tables 1 and 2).[20] Obviously, these distances are only indicative as they do not take into account possible steric hindrance and internal motion.

Examination of Fig. 2 and Table 1 shows that photolabels **2**–**5** fall into two categories. To the first one belongs photolabels **2** and **3**, characterized with long and flexible linkers, whose photo-cross-linking behaviour is reminiscent of ds^{4}U **1** with a larger exploration capacity. Whereas photolabels **4** and **5**, with short and more rigid linkers, constitute the second category to give cross-links which differ from those obtained with either **2**, **3** (at position 16.1) or ds^{4}U **1** (at position 1.1).

Position 16.1. Incorporation of the zero-length photo-cross-linker ds^{4}U **1** at position 16.1, prior to the cleavage site, yielded three cross-links with A2.1, U4 and U7.[7] The one with A2.1, unaccountable on the basis of the published structures,[2,9] and attributed to alternative conformations,[7] was not observed with any of photolabels **2**–**5**. However, the other two (with U4 and U7) were both detected with **2**–**5**:

- Since the long and flexible chains of **2** and **3** allowed s^{4}T to sweep the upper border of the catalytic pocket (C3, U4 and U7, G8), the absence of cross-link in its lower part (G5 and A6 forming the U-turn) is ascribed to the cross-linking polarity of the photolabel already observed in double stranded oligonucleotides.[14] Indeed, it has been shown that the photolabel which emerges from the helix major groove yielded cross-links with residues on the 3′- (but not 5′-) side of the strand bearing the photolabel.[14] Therefore, whereas A13 and A14 are accessible, residues G5 and A6 and those of helix III are not suitably disposed to be cross-linked.
- On the other hand, the shorter chain of **4** and **5** did not allow s^{4}T to reach C3 as observed above. The location of the pyrimidine C-5 atom into the major groove and the straight acetylenic bond bring the s^{4}T moiety of **5** into the vicinity of the GA mismatches. This might explain that, compared with **4**, a higher cross-linking yield was observed with G12 whose N-7;C-8 double bond is readily accessible. Photolabel **4** behaviour, with a short but rather flexible linker, is intermediate: its cross-linking pattern is similar to that of **5** with a higher photo-cross-linking yield with U7 as observed with **2** and **3**. All these cross-links, with the exception of those with A13, which will be discussed in more details below, are consistent with the published structures.

Position 1.1. Incorporation of ds^{4}U **1** at position 1.1, next to the cleavage site, yielded three cross-links with U4, G5 and A6 of the catalytic pocket. Two of them (with U4 and A6) could be explained on the basis of the published structures assuming a high mobility of residue 1.1 and/or of the catalytic loop.[7] The last one (with G5) is puzzling since (i) the inter-residue distance (12–13 Å) is larger than in the other cases; (ii) A6 is sandwiched between residue C17 and G5 in the 3D structure. However, these cross-links and

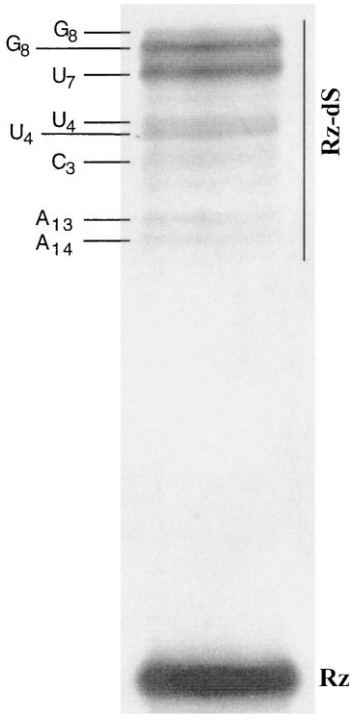

Figure 3. Electrophoretic separation on denaturing 15% polyacrylamide/8 M urea gel of the photo-cross-linked products (**Rz**–**dS**) obtained upon irradiation of **Rz** with **dS** containing **3** at position 16.1. Ribozyme residues involved in the cross-links are indicated.

others could be observed with **2** and **3** since their long and flexible linkers allow the photolabel to sweep not only the whole catalytic loop but also a large number of residues within helices I and II. On the other hand, **5** with its short and rigid side chain pointing towards the mismatch domain, yielded cross-links mainly with U7, G8 and G12. Molecular modelling shows that, when its linker is extended, **5** fills the gap between positions 1.1 and G8 whose orientation of the photo-reacting bonds is unfavourable (90° vs. an ideal value of 180°). Assuming that our proposed photochemical pathway involving the N-7;C-8 double bond of the purine is operating in the present case,[22] our observation highlights the dynamics of the system in solution with the mismatch domain undergoing reorientation to allow cross-link formation. The dynamics of the system is further illustrated by the photo-cross-links formed between **2** and **3** and residue A13 in the mismatch domain. These cross-links occurred whatever the substituted position (16.1 or 1.1) in substantial yield. Though they are compatible with the distances given in Table 1, it should be noted that (i) residue A13 is located on the opposite side of the mismatch and its access is

Table 2. Photo-cross-link data obtained when photolabels **1**,[7] **4** and **5** are inserted either at the 5′- or 3′-end of **dS**. For each labelled position, **Rz** cross-linked residues are reported in column 2; the overall and relative yields of cross-linking obtained with photolabels **1**, **4** and **5** are reported in columns 3–5. In the last two columns are reported the distances Å between both partner residues as determined from X-ray[2] (XR) or photolabelling derived molecular modelling[9] (*hν*) structures

Labelled position	Cross-linked residue	Photolabel			Distances Å	
		1	**4**	**5**	XR	*hν*
16.7	Overall yield	25	6	12		
	C15.6		60		7	7
	A15.7	100	40	100	5	5
1.6	Overall yield	8	3.8	2		
	AL2.4	45	6	10	25	9
	A2.6	55	94	90	5	5

Table 1. Photo-cross-link data obtained when photolabels **1**,[7] **2**–**5** are inserted either prior (16.1) or next (1.1) to the cleavage site of **dS**. For each labelled position, **Rz** cross-linked residues are reported in column 2; the overall and relative yields of cross-linking obtained with photolabels (**1**–**5**) are reported in columns 3–7. In the last two columns are reported the distances Å between both partner residues as determined from X-ray[2] (XR) or photolabelling derived molecular modelling[9] (*hν*) structures

Labelled position	Cross-linked residue	Photolabel					Distances Å	
		1	**2**	**3**	**4**	**5**	XR	*hν*
16.1	Overall yield	38	12	11	17	2		
	A2.1	37					19	20
	C2.2				3		21	22
	C3		2	7			17	18
	U4	11	6	10	18	13	14	14
	U7	**52**	**44**	**42**	**42**	14	5	5
	G8		38	24	20	28	7	9
	G12				17	**40**	10	9
	A13		3	4			11	10
	A14		3	6			9	9
1.1	Overall yield	40	8	7	10	5.5		
	C2.5		15	16		14	15	11
	C2.2		5	7	4		9	8
	C3		10	6	10		7	6
	U4	**48**	**18**	**24**	**25**	16	7	7
	G5	15	7	3			13	12
	A6	17	5	5			9	8
	U7		11	8	12	21	11	11
	G8		8	4	12	**25**	14	11
	G10.1		1.5				22	17
	C10.3		1	1.5			27	20
	G12					8	20	14
	A13		10	14			22	18

hindered by G8; (ii) according to the putative reaction mechanism, the formation of the cross-link might involve the N-7 atom of A13 which is engaged in an hydrogen bond stabilizing the mismatched A13:G8 base pair. This strongly suggests that this region is highly mobile.

Positions 1.6 and 16.7. The above results obtained with the four different labels introduced at positions 1.1 and 16.1 indicated a rather large dispersion of the cross-links when using those having 4-thiothymine at the end of a long chain. Accordingly, we reasoned that a higher selectivity should be observed with probes having labels **4** and **5** at positions 1.6 and 16.7. When position 16.7 was labelled with **5**, the sole cross-linked residue was A15.7 (as observed with **1**) while both A15.7 and C15.6 were cross-linked with **4** having a flexible side chain (Table 2). Cross-links were observed between the ends of stems I and II (with photolabels **1**, **4** or **5** placed at position 1.6), whereas none were detected between the ends of stem III and either stem I or II, thus further confirming the existence of the Y form in Mg^{2+} solutions.[10]

Conclusion

When photolabels **2**–**5** were inserted at a position, either prior or next to the cleavage site, the cross-linking results could be easily explained by analysis of the structures derived from the crystal or solution model studies. While most of the cross-linked sites were found in the catalytic loop, one notices that when using **2** and **3**, with long and flexible linkers allowing the 4-thiothymine to sweep a large domain, residues within helices I and II were reached. In contrast, photolabels **4** and **5**, with short and more rigid linkers, were shown to exhibit a higher selectivity. Moreover, unlike ds^{4}U **1**, both photolabels were able to cross-link residues involved in the double G:A mismatch. Short and rigid photolabels cross-linked residues G8 and/or G12, while long and flexible photolabels cross-linked A13. The latter result can be accommodated with the published structures if one assumes important local motions involving (i) opening the G8:A13 mismatch base pair which will give access of the 4-thiothymine to the N-7;C-8 double bond of A13; (ii) bringing this bond at a distance compatible with the linker length and taking into account the steric hindrance arising from the presence of G8 on the pathway followed by the photoreactive moiety. We thus suggested that, under cleavage conditions, the mismatch domain exhibits an unexpected high mobility.

Photolabel **1** has already been inserted in a cleavable deoxysubstrate analogue at the positions under study. It has been observed that none of the species containing a cross-link involving residues of the ribozyme core retained cleavage activity,[10] in contrast to those generated at the ends of helices I and III or between helices I and the loop closing helix II. The length and flexibility dependent photo-cross-linking ability of photolabels **2**–**5** can now be exploited to examine whether any of the cross-linked species retain cleavage activity as a consequence of enhanced conformational freedom. Work along these lines is in progress.

Experimental

General

Methyl thymin-1-ylacetate **6a**,[23] 5′-*O*-(4,4′-dimethoxytrityl)-5-iodo-2′-deoxyuridine 9,[16] 5′-*O*-[4,4′-dimethoxytrityl]-5-[3-methoxy-3-oxopropyl]-2′-deoxyuridine **11**[15] and 5′-*O*-[4,4′-dimethoxytrityl]-5-[3-[(2-amino)ethyl) amino]-3-oxopropyl]-2′-deoxyuridine **12a**[15] were synthesized following literature procedures. ^{1}H, ^{13}C, ^{31}P NMR spectra were recorded on Bruker AC 200, AC 250, AM 300 or AC 300-P spectrometers. ^{1}H chemical shifts (δ) are reported relative either to tetramethylsilane in $CDCl_3$ or residual solvent traces in CD_3OD (3.3 ppm) or in DMSO-d_6 (2.6 ppm). ^{13}C chemical shifts (δ) are reported relative to $CDCl_3$ (77.7 ppm) or to DMSO-d_6 (39.7 ppm). ^{31}P chemical shifts (δ) are reported relative to external 85% phosphoric acid. Interchangeable attributions are asterisked. Mass spectroscopy was carried out using AEI MS 50 (EI spectra) or AEI MS 9 (CI spectra) or Kratos MS 80 (HRMS, L-SIMS or FAB (thioglycerol matrix)) instruments. Tetrahydrofuran (THF), dichloromethane and dimethylformamide (DMF) were dried by heating, under reflux, with sodium/benzophenone, calcium hydride and barium oxide after azeotropic distillation with toluene, respectively. Acids, amines and 3′-OH nucleosides were dried at room temperature (RT) in a dessicator over phosphorus pentoxide under vacuum overnight before amide condensation and phosphitylation. Oligonucleotide syntheses were performed on an Applied Biosystems 392 synthesizer. Nucleoside β-cyanoethyl-phosphoramidites, columns and reagents were from PerSeptive Biosystems. All reactions were carried out at room temperature (RT) unless otherwise stated. Column chromatography was performed on Merck 7729 silica gel. Thin layer chromatography was run on precoated silica gel sheets with fluorescent indicator (254 nm) manufactured by Schleicher and Schuell (ref 394 732). Lichroprep RP 18 (Merk 13 900) was employed for reverse phase chromatography.

Methyl 4-thiothymin-1-ylacetate 6b. Methyl thymin-1-ylacetate **6a**[23] (9.92 g, 50 mmol) was dissolved in dioxane (250 mL) and the solution brought to reflux. Phosphorus pentasulfide (14.6 g, 1.3 equiv.) was then added and the mixture maintained to reflux for 1.5 h. After cooling to RT, the reaction mixture was filtered on Celite and the filtrate concentrated. Crystallization from methanol lead to 9.41 g of bright yellow crystals (88% yield). Recrystallization from ethanol gave an analytical sample. Mp: 176°C. ^{1}H NMR (200 MHz; DMSO-d_6), δ (ppm): 12.92 (s,1H, N^3–H), 7.80 (s, 1H, H6), 4.65 (s, 2H, N^1–CH_2), 3.80 (s, 3H, OCH_3), 2.05 (s, 3H, CH_3). ^{13}C NMR (50 MHz; DMSO-d_6), δ (ppm): 191.5 (C4), 168.4 (CO_2CH_3), 148.6 (C2), 139.2 (C6), 117.5 (C5), 52.6 (CO_2CH_3), 49.2 (N^1–CH_2), 16.7 (CH_3). CI-MS: *m/z* 215 $(M+H)^+$ HRMS (CI) calculated for $C_8H_{11}N_2O_3S$ 215.0490, found 215.0502. Calculated for $C_8H_{10}N_2O_3S$: C, 44.86; H, 4.71; N, 13.08; S, 14.94, found C, 45.14; H, 4.56; N, 13.07; S, 14.88.

4-Thiothymin-1-ylacetic acid 7. A suspension of methyl(4-thiothymin-1-yl)acetate **6b** (8.75 g, 41 mmol) in 2 N aqueous NaOH (50 mL) was submitted to sonication for 10 min. Then, the solution was chilled to 0°C, acidified to

pH 1 with 9.7N HCl and the resulting suspension filtered. The precipitate was washed with cold water and dried at RT in a dessicator over phosphorus pentoxide under vacuum to give 8.53 g of yellow crystals (96% yield). Mp: 228°C. ^{1}H NMR (300 MHz, DMSO-d_6), δ (ppm): 12.86 (s, 1H, N^3–H), 7.77 (s, 1H, H6), 4.53 (s, 2H, N^1–CH_2), 2.05 (s, 3H, CH_3). ^{13}C NMR (62 MHz, DMSO-d_6), δ (ppm): 191.5 (C4), 169.3 (COOH), 148.8 (C2), 139.6 (C6), 117.4 (C5), 49.4 (N^1–CH_2), 16.8 (CH_3). FAB$^+$-MS: *m/z* 201 $(M+H)^+$. Calculated for $C_7H_8N_2O_3S\cdot H_2O$: C, 38.53; H, 4.62; N, 12.84; S, 14.66; found C, 38.66; H, 4.48; N, 12.53; S, 14.65.

***S*-Pivaloyloxymethyl-4-thiothymin-1-ylacetic acid 8.** To a solution of **7** (2 g, 10 mmol) in dimethoxyethane (200 mL) was added K_2CO_3 (5.52 g, 4 equiv.), water (80 mL) and pivaloyloxylmethyl chloride (POMCl) (4.3 mL, 3 equiv.). The reaction was stirred at RT for 24 h then diluted with ethyl acetate (300 mL) and washed with 1N HCl. The aqueous phase was extracted twice with ethyl acetate. The combined organic layers were dried over sodium sulfate and concentrated. Crystallization of the residue from ethanol gave **13** as colourless crystals (2.25 g, 74% yield). Mp: 210°C. ^{1}H NMR (200 MHz, DMSO-d_6), δ (ppm): 7.96 (s, 1H, H6), 5.84 (s, 2H, CH_2 POM), 4.61 (s, 2H, N^1–CH_2), 2.04 (s, 3H, CH_3), 1.22 (s, 9H, CH_3 POM). ^{13}C NMR (50 MHz, DMSO-d_6), δ (ppm): 177.5 (C4), 174.2 (C=O POM), 169.3 (COOH), 153.3 (C2), 146.2 (C6), 110.2 (C5), 60.9 (CH_2 POM), 50.9 (N^1–CH_2), 38.4 ($C(CH_3)_3$ POM), 26.8 ($C(CH_3)_3$ POM), 13.2 (CH_3). CI-MS: *m/z* 315 $(M+H)^+$. HRMS (CI): calculated for $C_{13}H_{19}N_2O_5S$: 315.1014, found 315.1013. Calculated for $C_{13}H_{18}N_2O_5S$: C, 49.68; H, 5.77; N, 8.91; S, 10.18. Found: C, 49.66; H, 5.74; N, 8.84; S, 10.21.

5′-*O*-[4,4′-Dimethoxytrityl]-5-[(2-aminoethyl)amino]-2′-deoxyuridine 10. A solution of 5′-*O*-(4,4′-dimethoxytrityl)-5-iodo-2′-deoxyuridine **9**,[16] (1.35 g, 2.06 mmol) in freshly distilled ethylenediamine (3 mL) was stirred under argon for 40 h. The mixture was concentrated under reduced pressure to a gum that was purified by reverse phase chromatography (Lichroprep RP 18) using a gradient of CH_3CN in H_2O (0–100%) which afforded **10** (848 mg, 70% yield) as a foam. ^{1}H NMR (250 MHz, CD_3OD), δ (ppm): 7.50–7.16 (m, 9H, ar DMT), 6.85 (d, 4H, ar DMT, *J*=8.3 Hz), 6.62 (s, 1H, H_6), 6.40 (dd, 1H, H1′, *J*=6.2, 7.8 Hz), 4.44 (m, 1H, H3′), 3.98 (m, 1H, H4′), 3.76 (s, 6H, OCH_3 DMT), 3.46 (dd, 1H, H5′, *J*=3.0, 10.3 Hz), 3.24 (dd, 1H, H5″, *J*=3.7, 10.3 Hz), 2.42 (s, 4H, 2H 8 and 2H 9), 2.30 (m, 2H, H2′; H2″). ^{13}C NMR (50 MHz, $CDCl_3$), δ (ppm): 161.8 (C4), 159.2 (quat DMT), 149.8 (C2), 145.2 (quat DMT), 136.3 (quat DMT), 136.2 (quat DMT), 130.8 (ar DMT), 128.9 (ar DMT), 128.5 (ar DMT), 127.6 (ar DMT), 126.5 (C5), 113.8 (ar DMT), 111.1 (C6), 87.0 (quat DMT), 86.4 (C4′), 85.1 (C1′), 72.6 (C3′), 64.4 (C5′), 55.9 (OCH_3 DMT), 46.6 (C8*), 40.7 (C2′ and C9*). L-SIMS$^+$-MS: *m/z* 303 (DMT), 611 $(M+Na)^+$.

5′-*O*-[4,4′-Dimethoxytrityl]-5-[3-[(4-aminobutyl)amino]-3-oxopropyl]-2′-deoxyuridine 12b. A solution of 5′-*O*-[4,4′-dimethoxytrityl]-5-[3-methoxy-3-oxopropyl]-2′-deoxyuridine **11**[15] (100 mg, 0.162 mmol) in freshly distilled 1,4-diaminobutane (800 μL) was stirred under argon for 18 h. The mixture was concentrated under reduced pressure to a gum which was purified by reverse phase chromatography eluting with H_2O (50 mL), then 20% CH_3CN in H_2O (240 mL) affording **12b** (94 mg, 90% yield) as a foam. ^{1}H NMR (300 MHz, DMSO-d_6), δ (ppm): 7.77 (t, 1H, NH amide, *J*=5.4 Hz), 7.53–7.27 (m, 10H, H6; ar DMT), 6.98 (d, 4H, ar DMT, *J*=8.4 Hz), 6.26 (t, 1H, H1′, *J*=6.4 Hz), 4.31 (m, 1H, $H_{3'}$), 3.95 (m, 1H, $H_{4'}$), 3.83 (s, 6H, OCH_3 DMT), 3.28 (m, 2H, H5′; H5″), 3.06 (m, 2H, 2 H11), 2.60 (m, 2H, 2 H14), 2.43–2.17 (m, 6H, H2′; H2″; 2 H7 and 2 H8), 1.42 (m, 4H, 2 H12 and 2 H13). ^{13}C NMR (75 MHz, DMSO-d_6), δ (ppm): 170.9 (C9), 163.4 (C4), 158.3 (quat DMT), 150.5 (C2), 145.0 (quat DMT), 136.5 (C6), 135,7 (quat DMT), 129.9 (ar DMT), 128.0 (ar DMT), 127.8 (ar DMT), 126.9 (ar DMT), 113.4 (ar DMT), 113.1 (C5), 85.9 (quat DMT), 85.4 (C4′), 84.1 (C1′), 70.5 (C3′), 64.1 (C5′), 55.2 (OCH_3 DMT), 41.5 (C14), 39.4 (C2′), 38.5 (C11), 34.4 (C8), 30.7 (C12*), 26.8 (C13*), 23.0 (C7). FAB$^+$-MS: *m/z* 303 (DMT), 673 $(M+H)^+$, 695 $(M+Na)^+$.

***N*-Succinyl *S*-pivaloyloxymethyl-4-thiothymin-1-ylacetate 13.** *S*-pivaloyloxymethyl-4-thiothymin-1-ylacetic acid **8** was dissolved in THF (10 mL/mmol) and *N*-hydroxysuccinimide (1 equiv.) was added under a dry atmosphere. The reaction was chilled to 0°C and dicyclohexylcarbodiimide (1 equiv.) was added. After stirring overnight at 5°C, the resulting suspension was filtered. The filtrate was either used directly or the solvent evaporated to give a colourless powder which was used without purification for the next step.

General procedure for amide bond formation

To a THF solution of activated acid **13** (3 equiv.) under a dry atmosphere was added amine **10**, **12a**, **12b** or 3-aminopropyne and the reaction stirred at RT. Evolution of the reaction was monitored by TLC. The reaction mixture was diluted with CH_2Cl_2, the organic phase washed with a saturated sodium hydrogen carbonate solution, brine, dried over sodium sulfate and concentrated prior to purification by flash chromatography.

3-[(*S*-Pivaloyloxymethyl-4-thiothymin-1-ylacetyl)amino]-propyne 14. 3-Aminopropyne (210 μL, 3.77 mmol) treated with **13** as described in the general procedure gave after purification by flash chromatography (CH_3OH in CH_2Cl_2 0–2%) **14** (770 mg, 58% yield) as a foam. ^{1}H NMR (250 MHz, DMSO-d_6), δ (ppm): 8.81 (t, 1H, NH amide, *J*=5.3 Hz), 7.92 (s, 1H, H6), 5.84 (s, 2H, CH_2 POM), 4.54 (s, 2H, N^1–CH_2), 4.00 (dd, 2H, CH_2 prop, *J*=5.2, 2.4 Hz), 3.26 (t, 1H, H prop, *J*=2.4 Hz), 2.04 (s, 3H, CH_3), 1.22 (s, 9H, CH_3 POM). ^{13}C NMR (75 MHz, DMSO-d_6), δ (ppm): 177.5 (C4), 173.8 (C=O POM), 166.5 (C=O amide), 152.8 (C2), 146.8 (C6), 109.9 (C5), 80.8 (quat prop), 73.6 (CH prop), 60.9 (CH_2 POM), 51.6 (N^1–CH_2), 38.4 ($C(CH_3)_3$ POM), 28.3 (CH_2 prop), 26.8 ($C(CH_3)_3$ POM), 13.2 (CH_3). CI-MS: *m/z* 352 $(M+H)^+$. HR-MS (CI): found 352.1344, calculated for $C_{16}H_{22}N_3O_4S$ 352.1331.

5′-*O*-[4,4′-Dimethoxytrityl]-5-[3-[[2-[(*S*-pivaloyloxymethyl-4-thiothymin-1-ylacetyl)amino]ethyl]amino]-3-oxopropyl]-2′-deoxyuridine 15a. 5′-*O*-[4,4′-Dimethoxytrityl]-5-[3-[(2-amino)ethyl amino]-3-oxopropyl]-2′-deoxyuridine **12a**[15] (129 mg, 0.2 mmol) was treated with **13** as

described in the general procedure. Purification of the reaction product by flash chromatography (EtOH/CH_2Cl_2, 8:92, 1% TEA) gave **15a** (144 mg, 77% yield) as a foam. ^{1}H NMR (300 MHz, $CDCl_3$), δ (ppm): 7.87 (br s, 1H, NH amide), 7.55* (s, 1H, H6), 7.45–7.15 (m, 10H, H6″*; ar DMT), 7.03 (br s, 1H, NH amide), 6.83 (d, 4H, ar DMT, J=8.7 Hz), 6.34 (t, 1H, H1′, J=6.6 Hz), 5.77 (s, 2H, CH_2 POM), 4.54 (m, 3H, H3′; $N^{1″}$–CH_2), 4.06 (m, 1H, H4′), 3.77 (s, 6H, OCH_3 DMT), 3.45–3.26 (m, 6H, H5′; H5″; 2 H11; 2 H12), 2.50–2.14 (m, 6H, H2′; H2″; 2 H7 and 2 H8), 1.98 (s, 3H, CH_3), 1.16 (s, 9H, CH_3 POM). ^{13}C NMR (62 MHz, $CDCl_3$), δ (ppm): 179.0 (C4″), 176.7 (C=O POM), 173.6 (C9), 167.7 (C=O amide), 165.0 (C4), 159.3 (quat DMT), 155.3 (C2″), 151.3 (C2), 145.3 and 145.1 (C6″ and quat DMT), 138.0 (C6), 136.2 (quat DMT), 130.8 (ar DMT), 128.8 (ar DMT), 128.6 (ar DMT), 127.7 (ar DMT), 114.4 (C5″*), 113.9 (ar DMT), 113.0 (C5*), 87.4 (quat DMT), 86.8 (C4′), 85.6 (C1′), 72.8 (C3′), 64.5 (C5′), 61.4 (CH_2 POM), 55.9 (OCH_3 DMT), 53.2 ($N^{1″}$-CH_2), 41.4 (C2′), 40.4–39.5 and 39.4 ($C(CH_3)_3$ POM; C11 and C12), 36.3 (C8), 27.6 ($C(CH_3)_3$ POM), 23.7 (C7), 14.4 (CH_3). FAB$^+$-MS: m/z 303 (DMT), 653 (M+Na−312+1)$^+$, 675 (M−1+2Na−312+1)$^+$, 963 (M+Na)$^+$.

5′-*O*-[4,4′-Dimethoxytrityl]-5-[3-[[4-[(*S*-pivaloyloxymethyl-4-thiothymin-1-ylacetyl)amino]butyl]amino]-3-oxopropyl]-2′-deoxyuridine 15b. Nucleoside **12b** (500 mg, 74 mmol) was treated with **13** as described in the general procedure. Purification of the reaction product by flash chromatography (MeOH/CH_2Cl_2, 6:94, 1% TEA), gave **15b** (240 mg, 34% yield) as a foam. ^{1}H NMR (300 MHz, $CDCl_3$), δ (ppm): 7.72 (br s, 1H, NH amide), 7.51 (s, 1H, H6″*), 7.46–7.14 (m, 10H, H6*; ar DMT), 6.83 (d, 4H, ar DMT, J=8.5 Hz), 6.56 (br s,1H, NH amide), 6.37 (t, 1H, H1′, J=6.6 Hz), 5.78 (s, 2H, CH_2 POM), 4.52 (m, 3H, $N^{1″}$–CH_2 and H3′), 4.08 (m, 1H, H4′), 3.76 (s, 6H, OCH_3 DMT), 3.43–3.06 (m, 6H, 2 H11; 2 H14; H5′ and H5″), 2.50–2.10 (m, 6H, H2′; H2″; 2 H7 and 2 H8), 1.99 (s, 3H, CH_3), 1.60–1.34 (m, 4H, 2 H12 and 2 H13), 1,16 (s, 9H, CH_3 POM). ^{13}C NMR (75 MHz, $CDCl_3$), δ (ppm): 179.0 (C4″), 176.4 (C=O POM), 172.8 (C9), 167.3 (C=O amide), 164.7 (C4), 159.1 (quat DMT), 155.2 (C2″), 151.3 (C2), 145.4 (C6″), 145.1 (quat DMT), 137.8 (C6), 136.1 (quat DMT), 130.6 (ar DMT), 128.7 (ar DMT), 128.5 (ar DMT), 127.5 (ar DMT), 114.0 (C5*), 113.8 (ar DMT), 112.8 (C5″*), 87.1 (quat DMT), 86.6 (C4′), 85.3 (C1′), 72.4 (C3′), 64.4 (C5′), 61.3 (CH_2 POM), 55.8 (OCH_3 DMT), 53.1 ($N^{1″}$–CH_2), 41.0 (C2′), 39.9; 39.4; 39.3 (C11; C12; $C(CH_3)_3$ POM), 35.6 (C8), 27.4 ($C(CH_3)_3$ POM), 27.1 and 26.8 (C12 and C13), 23.9 (C7), 14.2 (CH_3). FAB$^+$-MS: m/z 303 (DMT), 681 (M+Na−312+1)$^+$, 703 (M−1+2Na−312+1)$^+$, 991 (M+Na)$^+$.

5′-*O*-[4,4′-Dimethoxytrityl]-5-[[2-[(*S*-pivaloyloxymethyl-4-thiothymin-1-ylacetyl)amino]ethyl]amino]-2′-deoxyuridine 16. Nucleoside **10** (74 mg, 0.13 mmol) was treated with **13** as described in the general procedure. Purification of the reaction product by flash chromatography (MeOH/CH_2Cl_2, 0–5%, 1% TEA), gave nucleoside **16** (60 mg, 54% yield) as a foam. ^{1}H NMR (250 MHz, $CDCl_3$), δ (ppm): 7.64 (br s, 1H, NH amide), 7.50–7.10 (m, 10H, H6″; ar DMT), 6.81 (d, 4H, ar DMT, J=7.2 Hz), 6.52 (s, 1H, H6), 6.46 (t, 1H, H1′, J=6.6 Hz), 5.78 (s, 2H, CH_2 POM), 4.55 (s, 2H, $N^{1″}$–CH_2), 4.44 (m, 1H, H3′), 4.06 (m, 1H, H4′), 3.76 (s, 6H, OCH_3 DMT), 3.50–3.00 (m, 6H, H5′; H5″; 2 H8; 2 H9), 2.37 (m, 2H, H2′; H2″), 1.99 (s, 3H, CH_3), 1.15 (s, 9H, CH_3 POM). ^{13}C NMR (62 MHz, $CDCl_3$), δ (ppm): 179.0 (C4″), 176.7 (C=O POM), 168.1 (C=O amide), 161.4 (C4), 159.2 (quat DMT), 155.3 (C2″), 149.5 (C2), 145.5 (C6″), 145.1 (quat DMT), 136.2 (quat DMT), 136.1 (quat DMT), 130.8 (ar DMT), 128.8 (ar DMT), 128.6 (ar DMT), 127.7 (ar DMT), 126.0 (C5), 113.8 (ar DMT), 113.0 (C5″), 111.6 (C6), 87.0 (quat DMT), 86.5 (C4′), 85.2 (C1′), 72.7 (C3′), 64.5 (C5′), 61.3 (CH_2 POM), 55.9 (OCH_3 DMT), 53.9 ($N^{1″}$–CH_2), 40.6 (C2′*), 39.5 (C8; C9; $C(CH_3)_3$ POM*), 14.4 (CH_3). FAB$^+$-MS: m/z 303 (DMT); 653 (M+Na−255+1)$^+$; 675 (M−H+2Na−255+1)$^+$, 789 (M+Na−119+1)$^+$, 907 (M+Na)$^+$.

5′-*O*-[4,4′-Dimethoxytrityl]-5-[3-[(*S*-pivaloyloxymethyl-4-thiothymin-1-ylacetyl)amino]prop-1-yn-1-yl]-2′-deoxyuridine 17. To a solution of 5′-*O*-(4,4′-dimethoxytrityl)-5-iodo-2′-deoxyuridine **9**[16] (374 mg, 0.57 mmol) in DMF (4 mL) was added CuI (26 mg, 0.24 equiv.), Et_3N (150 μL, 2 equiv.) and compound **14** (400 mg, 2 equiv.). The reaction was degassed then purged under argon and $(Ph_3P)_4Pd(0)$ (80 mg, 0.12 equiv.) was added and the reaction again purged with argon and stirred for 6.5 h. The reaction was concentrated, diluted with ethyl acetate (50 mL) and the organic phase washed with 3×25 mL of a saturated hydrogen carbonate solution and dried over sodium sulfate. Then it was concentrated and the residue chromatographed on silica gel column eluting with a gradient of 0–10% of methanol in CH_2Cl_2 to afford **17** (223 mg, 44% yield) as a foam. ^{1}H NMR (300 MHz, DMSO-d_6), δ (ppm): 11.82 (s, 1H, *N*3-H), 8.85 (t, 1H, NH amide, J=4.8 Hz), 8.08 (s, 1H, H6″), 7.94 (s, 1H, H6), 7.64–7.31 (m, 9H, ar DMT), 7.02 (d, 4H, ar DMT, J=8.3 Hz), 6.24 (t, 1H, H1′, J=6.5 Hz), 5.88 (s, 2H, CH_2 POM), 5.47 (d, 1H, OH 2′, J=4.3 Hz), 4.57 (s, 2H, $N^{1″}$–CH_2), 4.39 (m, 1H, H3′), 4.06 (m, 3H, H4′; 2 H9), 3.84 (s, 6H, OCH_3 DMT), 3.38 (dd, 1H, H5′, J=10.2, 5.3 Hz), 3.20 (br d, 1H, H5″, J=10.2 Hz), 2.35 (m, 2H, H2′;H2″), 2.05 (s, 3H, CH_3), 1.24 (s, 9H, CH_3 POM). ^{13}C NMR (75 MHz, DMSO-d_6), δ (ppm): 177.5 (C4″), 173.7 (C=O POM), 166.3 (C=O amide), 161.7 (C4), 158.2 (quat DMT), 153.2 (C2″), 149.5 (C2), 146.8 (C6″), 145.0 (quat DMT), 143.7 (C6), 135.8 (quat DMT), 135.4 (quat DMT), 129.8 (ar DMT), 128.0 (ar DMT), 127.7 (ar DMT), 126.8 (ar DMT), 113.4 (ar DMT), 109.8 (C5″), 98.3 (C5), 89.0 (C7), 86.0 (quat DMT; C4′), 85.2 (C1′), 74.7 (C8), 70.6 (C3′), 63.9 (C5′), 60.8 (CH_2 POM), 55.2 (OCH_3 DMT), 51.4 ($N^{1″}$–CH_2), 40.0 (C2′), 38.3 ($C(CH_3)_3$POM), 29.0 (C9), 26.7 ($C(CH_3)_3$POM), 13.2 (CH_3). FAB$^+$-MS: m/z 902, (M+Na)$^+$.

Preparation of phosphoramidites 18a, 18b, 19, 20. To a solution of each nucleoside (**15a**, **15b**, **16** and **17**) in CH_2Cl_2 (8.9 mL/mmol) under argon, was added *N*,*N*-diisopropylethylamine (4 equiv.) and 2-cyanoethyl *N*,*N*-diisopropylchloro-phosphoramidite (3 equiv.). Upon completion of the reaction, the mixtures were concentrated and the residues dissolved in CH_2Cl_2. The solutions were washed with sodium hydrogen carbonate, dried over sodium sulfate and the desired products (**18a**, **18b**, **19** and **20**) characterized. ^{31}P NMR (121.49 MHz, $CDCl_3$): δ ppm

18a: 149.5–149.3 ppm, **18b**: 149.7–149.5 ppm, **19**: 149.5–149.1 ppm, **20**: 149.6–149.3 ppm.

Photolabelled deoxysubstrate analogues and ribozyme synthesis

Synthesis of all **dS** were carried out using conventional phosphoramidite chemistry.[24] In the case of substrate analogues with the label in position 1.6, a 15-mer bearing an extra A in position 1.7 was synthesized. Sequences were prepared on a 1 μmol scale using the trityl off end procedure and employing the standard DNA synthesis cycle provided by Applied Biosystems. Modified 2′-deoxyuridine phosphoramidites (**18a**, **18b**, **19** and **20**) were used as 0.1 M acetonitrile solutions. Coupling time for their incorporation was extended to 10 min. After synthesis, the solid supports were treated at room temperature with NH_4OH 33% for two days, then the solutions were concentrated to dryness. Complete purification of the oligomers was performed in two steps: first truncated oligonucleotides were separated from the full-length oligomers by gel electrophoresis on a denaturing 20% polyacrylamide gel; then thiolated-oligomers were separated from non-thiolated ones on an affinity gel slowing down the desired oligomers.[25]

Rz ribozyme was synthesized either chemically (see above, deprotection was accomplished with NH_4OH 33%/EtOH 2:1) or by in vitro transcription. In this latter case transcription was effectued by T7 RNA polymerase in the presence of α-^{32}P-dCTP and synthetic single strand DNA templates that are double-stranded at the promoter site. The products were isolated by running on 15% PAGE-8 M urea. The bands of interest were cut, eluted, precipitated and quantified by Cerenkov counting. The ribozyme transcripts were dephosphorylated using Calf Intestine Alkaline Phosphatase: 30 min at 37°C, 15 min at 45°C (in order to expose the 5′ extremity) and finally 30 min at 37°C with a new equivalent of CIP. Then the mixture was treated with 10 units of Proteinase K in the presence of 2% SDS. After phenol extraction, ribozyme was precipitated and then ^{32}P-labelled at the 5′-end as previously described.[19] The only difference between these two methods of ribozyme synthesis being that ribozyme obtained by enzymatic synthesis contains an extra G residue at its 5′-end. Photolabelling studies realized with these two kind of ribozyme yielded the same results.

Ribozyme photolabelling studies

Oligodeoxynucleotides **dS** (1.2 μM) were placed in 50 mM Tris–HCl pH 8, 0.5 mM EDTA and 20 mM $MgCl_2$ in the presence of 5′-^{32}P-labelled ribozyme (0.2 μM).[19] Each sample (5 μL) was introduced in a siliconized glass capillary and placed 5 cm from the exit slit of a Bausch and Lomb monochromator equipped with a HBO 200 W superpressure mercury lamp and a Schott WG 345 filter. The samples thermostated at 15°C were irradiated at 366 nm during 45 min. (Total fluence=200 kJ/m^2.) Large gels (40 cm) were used to separate multiple cross-linked species on 15% PAGE-8 M urea. Cross-linked and non-cross-linked species were detected by autoradiography, excised, quantified by Cerenkov counting and by phosphorimager (Molecular Dynamics), eluted and precipitated. Localization of the RNA cross-links was achieved by limited alkaline hydrolysis as previously described.[19]

Acknowledgements

We are indebted to Dr M. Thomas for the chemical synthesis of all-deoxy ribozyme substrate analogues **dS** and ribozyme **Rz**. This work was supported by grants of Ligue Nationale contre le Cancer and ANRS.

References

1. (a) Vaish, N. K.; Kore, A. R.; Eckstein, F. *Nucleic Acids Res.* **1998**, *26*, 5237–5242. (b) Eckstein, F., Lilley, D. M. J., Eds. 1997, *Catalytic RNA*; Springer: Berlin. (c) Burlina, F.; Favre, A.; Fourrey, J.-L. *Bioorg. Med. Chem.* **1997**, *5*, 1999–2010.
2. (a) Wedekind, J. E.; McKay, D. B. *Annu. Rev. Biomol. Struct.* **1998**, *27*, 475–502. (b) Scott, W. G.; Finch, J. T.; Klug, A. *Cell* **1995**, *81*, 991–1002. (c) Pley, H. W.; Flaherly, K. M.; McKay, D. B. *Nature* **1994**, *372*, 68–74.
3. (a) Bassi, G. S.; Mollegaard, N. E.; Murchie, A. I. H.; Lilley, D. M. *J. Biochem.* **1999**, *38*, 3345–3354. (b) Bassi, G. S.; Mollegaard, N. E.; Murchie, A. I. H.; Kitzing, E.; Lilley, D. M. *J. Nature Struct. Biol.* **1995**, *2*, 45–55.
4. Amiri, K. M. A.; Hagerman, P. J. *Biochemistry* **1994**, *33*, 13172–13177.
5. Tuschl, T.; Gohlke, C.; Jovin, T. M.; Westhof, E.; Eckstein, F. *Science* **1994**, *266*, 785–789.
6. (a) Zhou, D.-M.; He, Q.-C.; Zhou, J.-M.; Taira, K. *FEBS Lett.* **1998**, *431*, 154–160. (b) van Tol, H.; Buzayan, J. M.; Felstein, F.; Eckstein, F.; Bruening, G. *Nucleic Acids Res.* **1990**, *18*, 1971–1975.
7. Woisard, A.; Fourrey, J.-L.; Favre, A. *J. Mol. Biol.* **1994**, *239*, 366–370.
8. Woisard, A.; Favre, A.; Clivio, P.; Fourrey, J.-L. *J. Am. Chem. Soc.* **1992**, *114*, 10072–10073.
9. Laugâa, P.; Woisard, A.; Fourrey, J.-L.; Favre, A. *C. R. Acad. Sci., Life Sci.* **1995**, *318*, 307–313.
10. Bravo, C.; Woisard, A.; Fourrey, J.-L.; Laugâa, P.; Favre, A. *Biochimie* **1999**, *81*, 201–212.
11. Scott, W. G.; Murray, J. B.; Arnold, J.; Stoddard, B. L.; Klug, A. *Science* **1996**, *274*, 2065–2069.
12. (a) Murray, J. B.; Terwey, D. P.; Maloney, L.; Karpeisky, A.; Usman, N.; Beigelman, L.; Scott, W. G. *Cell* **1998**, *92*, 665–673. (b) Peracchi, A.; Beigelman, L.; Scott, E. C.; Uhlenbeck, O. C.; Herschlag, D. *J. Biol. Chem.* **1997**, *272*, 26822–26826.
13. Saintomé, C.; Clivio, P.; Fourrey, J.-L.; Woisard, A.; Favre, A. *Tetrahedron Lett.* **1994**, *35*, 873–876.
14. Saintomé, C.; Clivio, P.; Favre, A.; Fourrey, J.-L.; Laugâa, P. *J. Chem. Soc., Chem. Commun.* **1997**, 167–168.
15. Dreyer, G. B.; Dervan, P. B. *Proc. Natl. Acad. Sci. U.S.A.* **1985**, *82*, 968–972.
16. Crouch, G. J.; Eaton, B. E. *Nucleosides Nucleotides* **1994**, *13*, 939–944.
17. Hobbs, F. W. *J. Org. Chem.* **1989**, *54*, 3420–3422.
18. Tong, G.; Lawlor, J. M.; Tregear, G. W.; Haralambidis, J. *J. Org. Chem.* **1993**, *58*, 2223–2231.
19. Dos Santos, D. V.; Vianna, A.-L.; Fourrey, J.-L.; Favre, A. *Nucleic Acids Res.* **1993**, *21*, 201–207.
20. Molecular graphics were displayed on a Silicon Graphics O2

R10000 workstation. Building, measurements and conformational analysis were performed using SYBYL package (Tripos). The conformational space accessible to the s^4T moiety of **2**–**5** was explored via systematic search, performed along the torsional angles of the linker.

21. Favre, A.; Fourrey, J. -L. *Acc. Chem. Res.* **1995**, *28*, 375–382.
22. (a) Saintomé, C.; Clivio, P.; Favre, A.; Fourrey, J.-L. *J. Org. Chem.* **1997**, *62*, 8125–8130. (b) Saintomé, C.; Clivio, P.; Fourrey, J.-L.; Favre, A.; Riche, C. *J. Am. Chem. Soc.* **1996**, *118*, 8142–8143.
23. Egholm, M.; Buchardt, O.; Nielsen, P. E.; Berg, R. H. *J. Am. Chem. Soc.* **1992**, *114*, 1895–1897.
24. Beaucage, S.; Iyer, R. P. *Tetrahedron* **1993**, *48*, 2223–2311.
25. (a) Lemaigre-Debreuil, Y.; Expert-Bezançon, A.; Favre, A. *Nucleic Acids Res.* **1991**, *19*, 3653–3660. (b) Igloï, G. L. *Biochemistry* **1988**, *27*, 3842–3849.